

Position Aided Beam Prediction in the Real World: How Useful GPS Locations Actually Are?

João Morais¹, Arash Behboodi², Hamed Pezeshki² and Ahmed Alkhateeb¹

¹ Wireless Intelligence Lab, Arizona State University, USA - Emails: {joao, alkhateeb}@asu.edu

² Qualcomm Research, USA - Emails: {behboodi, hamedp}@qti.qualcomm.com

Abstract—Millimeter-wave (mmWave) communication systems rely on narrow beams for achieving sufficient receive signal power. Adjusting these beams is typically associated with large training overhead, which becomes particularly critical for highly-mobile applications. Intuitively, since optimal beam selection can benefit from the knowledge of the positions of communication terminals, there has been increasing interest in leveraging position data to reduce the overhead in mmWave beam prediction. Prior work, however, studied this problem using only synthetic data that generally does not accurately represent real-world measurements. In this paper, we investigate position-aided beam prediction using a real-world large-scale dataset to derive insights into precisely how much overhead can be saved in practice. Furthermore, we analyze which machine learning algorithms perform best, what factors degrade inference performance in real data, and which machine learning metrics are more meaningful in capturing the actual communication system performance.

I. INTRODUCTION

To unlock the exorbitant data rates only possible with multiple GHz of bandwidth of MmWave and THz frequencies, mobile communications systems are envisioned to use large antenna arrays and rely mainly on Line-of-sight (LOS) links [1]. In order to optimally oriented the narrow beams of such arrays, systems incur in high overhead. Current systems use spectrum to perform channel measurements, which motivates an important question: Can communication systems derive channel knowledge by means that do not involve the expenditure of resources useful for communication? The LOS dependency at these frequencies has motivated academia to consider using data on the position of connected devices to aid the system in spatial multiplexing decision-making, but real-world studies are scarce. In this direction, this paper uses real-world measurements with GPS position and mmWave data to assess how much signaling overhead can be reduced.

Using GPS positions to reduce the overhead of beam management is not a new idea [2]–[4]. However, to the authors’ knowledge, it is yet to be assessed in real-world scenarios. For example, in [2], the authors simulate an adaptive beamwidth approach on ray-tracing data to cope with variable UE-BS distances. Likewise, the work in [3] uses a deep neural network on synthetic position and orientation data of the UE to reduce the beam alignment overhead. Using also computer-generated data, [5] and [4] assess GPS inaccuracies by introducing noise in position measurements, achieving 85–90% alignment probability. Given these promising results, it is important to question whether similar accuracies would be achieved in the real-world using practical GPS and mmWave

communication systems. This paper attempts to answer this important question.

It may seem straightforward to decide on which beams the BS should use from GPS positions of the, especially for line-of-sight (LOS) scenarios. But that is only true in simulations with ideal/synthetic data. Although utilizing GPS positions can still make a sizable difference, it is crucial to know how reality varies from simulation. To that end, we show beam prediction performances obtained through real-world data, and attempt to answer the following questions:

- How much overhead in beam training can we save by predicting beams based on GPS positions?
- How is the performance of neural networks compared to more classical machine learning solutions for the position-aided beam prediction task?
- What factors degrade the performance of position-aided beam alignment methods in real-world data?
- What are the good metrics for evaluating the performance of the beam prediction machine learning models?

We present the accuracies for position-aided beam prediction for a broad set of real-world scenarios, belonging to the DeepSense dataset [6]. All simulation code is available in [7].

To answer the questions above, we first describe a system model and formulate the beam prediction problem in Section II. We propose ML-based solutions in Section III. Then in Section IV, we describe our real-world data collection and how data is pre-processed in this work. Section V answers all questions above. Finally, Section VI summarizes the most important findings on position-aided beam prediction.

II. SYSTEM MODEL AND PROBLEM FORMULATION

In this section, we formally state the system model and assumptions, as well as define the beam prediction problem.

A. System Model

We consider a system where a BS with N antennas communicates with a single-antenna user equipment (UE). The BS can transmit/receive information to/from the UE using any of the M beamforming vectors $\mathbf{f}_m \in \mathbb{C}^{N \times 1}$ present in its codebook $\mathcal{F} = \{\mathbf{f}_m\}_{m=1}^M$. If x is the complex symbol transmitted by the BS using the beamformer \mathbf{f}_m , the received symbol in the downlink is given by

$$y = \mathbf{h}^T \mathbf{f}_m x + n, \quad (1)$$

where $\mathbf{h} \in \mathbb{C}^{N \times 1}$ is the complex channel vector that holds the amplitude and phase transformations that occur between each BS antenna and the UE antenna, and $n \sim \mathcal{N}_{\mathbb{C}}(0, \sigma^2)$ represents complex normally distributed noise.

B. Problem Formulation

Adopting receive power as a performance metric, optimal beam selection occurs when the BS picks the beamformer that results in the highest received power $P = \mathbb{E} \left[|y|^2 \right]$. Formally, the ideal beamformer \mathbf{f}^* can be obtained using

$$\mathbf{f}^* = \underset{\mathbf{f} \in \mathcal{F}}{\operatorname{argmax}} \left| \mathbf{h}^T \mathbf{f} \right|^2. \quad (2)$$

In this work, instead of relying on the explicit channel knowledge, i.e., the knowledge of \mathbf{h} , which is hard to acquire, we target predicting the optimal beam based solely on the real-time position information of the UE. If $\mathbf{g} \in \mathbb{R}^2$ denotes the two-dimensional position vector, composed of latitude g_{lat} and longitude g_{long} , our problem consists in approximating \mathbf{f}^* by the estimation $\hat{\mathbf{f}}$ that maximizes $\mathbb{P}(\hat{\mathbf{f}} = \mathbf{f}^* | \mathbf{g})$.

III. POSITION-AIDED BEAM PREDICTION: PROPOSED MACHINE LEARNING SOLUTIONS

Leveraging position for beam prediction is motivated by the directional nature of the narrow beams at mmWave and the higher dependency on Line-of-sight (LOS) paths. The mapping relation (function) between the position and the best beam could arguably be learned using prior observations of position-beam pairs, for example at the infrastructure. In this section we first introduce our problem in light of ML approaches, then we present and justify the choices for such approaches, carefully detailing how they work.

We approximate \mathbf{f}^* through a prediction function $f_{\Theta}(\mathbf{g})$ parameterized by a set Θ that represents the parameters of the model. The parameters Θ are learned from a dataset $\mathcal{D} = \{(\mathbf{g}_k, \mathbf{f}_k^*) : k = 1, \dots, K\}$ which is composed of K labeled training samples. Each sample consists of the input location \mathbf{g}_k and its ground truth optimal beamforming vector $\mathbf{f}_k^* \in \mathcal{F}$. Therefore, for a given position \mathbf{g} we have $\hat{\mathbf{f}} = f_{\Theta}(\mathbf{g})$.

The internal behavior of f_{Θ} depends on our learning strategy. We use three approaches, respectively, based on a lookup table (LT), K-nearest neighbors (KNN), and a fully connected neural network (NN). The lookup table and KNN approaches represent attractive choices due to their simple and intuitive nature while implicitly integrating spatial correlation knowledge, i.e., they assume similar LOS positions should have similar optimal beams. Lastly, although neural networks have higher complexity, they are powerful inference systems, which can be useful in learning from position data.

All three algorithms estimate a probability distribution $\mathcal{P} \in \{p_1, \dots, p_M\}$, where $p_m = \mathbb{P}(\mathbf{f}_m = \mathbf{f}^*)$. The beamformer with highest probability is chosen:

$$\hat{\mathbf{f}} = \mathbf{f}_{\hat{m}}, \quad \hat{m} = \underset{m \in \{1, \dots, M\}}{\operatorname{argmax}} p_m. \quad (3)$$

We proceed to describe how each beam prediction approach derives the probability vector \mathcal{P} .

A. Lookup Table

This approach is motivated by the intuition that a beam covers at least one contiguous physical area. So, we discretize the input space into small areas or cells and attribute a beam to each one. More specifically, given a position \mathbf{g} , with each coordinate normalized between 0 and 1, we apply a mapping function $Q(\mathbf{g})$ to find in which cell of a uniform square 2D grid the position falls into. The quantization/cell-mapping function $Q(\mathbf{g})$ that maps positions to 2D cells with area inversely proportional to the number of cells, N_{lt} , is given by:

$$Q(\mathbf{g}) = (q_{row}, q_{col}) = \left(\left\lfloor g_{lat} \sqrt{N_{lt}} \right\rfloor, \left\lfloor g_{lon} \sqrt{N_{lt}} \right\rfloor \right). \quad (4)$$

After knowing the cells each training sample belongs to, we attribute a beam to each cell based on the mode of beam reports. In essence, the best beam that is most commonly reported is taken as the top-1 prediction for input positions in that cell, the second most reported beam as top-2, etc. If a cell does not have any training data, the algorithm predicts randomly, and this becomes more likely as N_{lt} increases and cells get smaller. See Alg. 1 for a detailed description.

Algorithm 1 Lookup Table

Require: \mathbf{g} , $\mathcal{D} = \{(\mathbf{g}_k, \mathbf{f}_k^*)\}$, $N_{lt} \geq 1$

```

for  $q \leftarrow 1$  to  $N_{lt}$  do
   $\mathcal{U} \leftarrow \{k : q = Q(\mathbf{g}_k)\}$            ▷ Find samples in cell  $q$ 
   $N_q \leftarrow \# \mathcal{U}$                        ▷ Count samples in cell  $q$ 
  if  $N_q = 0$  then                       ▷ If no samples in cell  $q$ 
     $\mathcal{P}_q = \{p_m = 1/M\}_{m=1}^M$          ▷ Predict randomly
  continue                               ▷ Continue to next cell
   $\mathcal{F}_{lt} \leftarrow \{\mathbf{f}_{u_t}^* : u_t \in \mathcal{U}\}_{t=1}^{N_q}$    ▷ Get labels in cell  $q$ 
  for  $m \leftarrow 1$  to  $M$  do
     $o_m \leftarrow 0$ 
    for  $f \in \mathcal{F}_{lt}$  do ▷ Count occurrences of  $f_m$  in  $\mathcal{F}_{lt}$ 
      if  $f = \mathbf{f}_m$  then
         $o_m \leftarrow o_m + 1$ 
     $\mathcal{P}_q \leftarrow \{p_m = o_m/N\}$        ▷ Compute probabilities
   $q \leftarrow Q(\mathbf{g})$                  ▷ Find cell of input position
   $\mathcal{P} \leftarrow \mathcal{P}_q$                    ▷ Get prediction for that cell

```

B. K-Nearest Neighbors

The rationale behind KNN is that similar/neighbor positions should have similar beams. We first identify the N_{knn} nearest neighbors. The selected neighbors then report their best beam. We take the mode of those reports as our best beam estimation. See Alg. 2 for the detailed steps.

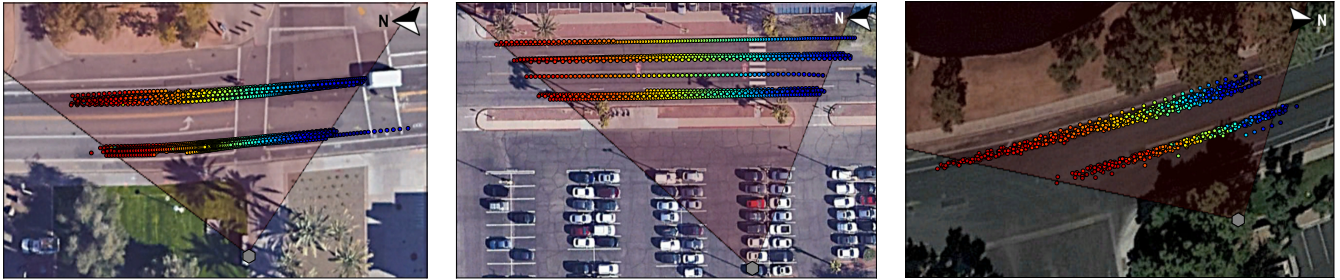
Algorithm 2 K-Nearest Neighbors

Require: \mathbf{g} , $\mathcal{D} = \{(\mathbf{g}_k, \mathbf{f}_k^*)\}$, $N_{knn} \geq 1$

```

 $\{d_k \leftarrow |\mathbf{g}_k - \mathbf{g}|\}_{k=1}^K$        ▷ distances to all training samples
Let  $\{u_n\}_{n=1}^{N_{knn}}$  be the indices of the  $N_{knn}$  smallest distances
 $\mathcal{F}_{knn} \leftarrow \{\mathbf{f}_{u_n}^*\}_{n=1}^{N_{knn}}$    ▷ Get the labels for closest neighbors
Let  $\{o_m\}_{m=1}^M$  be the number of occurrences of  $f_m$  in  $\mathcal{F}_{knn}$ 
 $\mathcal{P} \leftarrow \{p_m = o_m/N\}$ 

```



(a) Scenario 1 [2667 datapoints]

(b) Scenario 6 [1011 datapoints]

(c) Scenario 7 [897 datapoints]

Fig. 1. Color-coded data representation, best beam versus position. The red area represents the Field of View of the RGB camera modality (not used).

C. Neural Network

We use a standard fully-connected NN setup. The architecture and main hyperparameters are present in Table I. We found this architecture to be the inflection point after which further increasing the model complexity leads to no returns. Note that one hidden layer with 128 nodes gets us just 2.5% less accuracy on average. Therefore, we are certain this network size is not limiting our results.

For NN training, after training for 60 epochs, we see in which epoch the network had the highest accuracy on the validation set and use that model to assess accuracy on the test set. We use cross-entropy loss and tune the neural network weights with Adam optimizer [8]. The initial learning rate provided to Adam is 0.01 and we use a multi-step learning rate scheduler that multiplies all learning parameters by 0.2 at epochs 20 and 40. Finally, as an additional pre-processing step for the neural network, we quantized the input data in 200 bins, i.e., a resolution of 0.005 considering the normalized input has values between zero and one.

IV. MEASUREMENTS AND DATASET DESCRIPTION

The data used in this work is part of DeepSense¹ [6], an extensive multi-modal real-world dataset constructed by the Wireless Intelligence Lab. The dataset merges co-existing GPS locations, camera images, radar, lidar, and beam-training power/CSI measurements in each data point. For this work, we use the calibrated GPS positions and power data of DeepSense Scenarios 1 to 9. This section presents how the dataset was acquired and what pre-processing steps we performed on it.

A. Data acquisition

DeepSense contains data acquired on different locations around the ASU campus, day and night. The UE is equipped with a GPS inside a moving car and a mmWave omnidirectional transmitter operating at 60 GHz. The BS is fixed and is equipped with a mmWave receiver. The BS uses a uniform square array with 64 antenna elements. The car passes several times in front of the BS, in different directions. At a rate of ten times a second, the BS sweeps the codebook \mathcal{F} and collects the powers it received in each beam. In Figure 1, we show for some Scenarios a GPS image from above, and a

¹Datasets were downloaded and evaluated by ASU researchers.

TABLE I
ARCHITECTURE AND TRAINING HYPER-PARAMETERS

Parameters	Values
Input size	2 (g_{lat} and g_{long})
Hidden Layers	3 layers, 256 nodes each
Output size	$M \in \{8, 16, 32, 64\}$
Activation	ReLU on hidden layers
Training Batch Size	32
Learning Rate	1×10^{-2}
Learning Rate Decay	epochs 20 and 40
Learning Rate Reduction Factor	0.2
Total Training Epochs	60

scatter plot of positions, where color indicates the best beam (out of 64 beams) for that position.

B. Data normalization

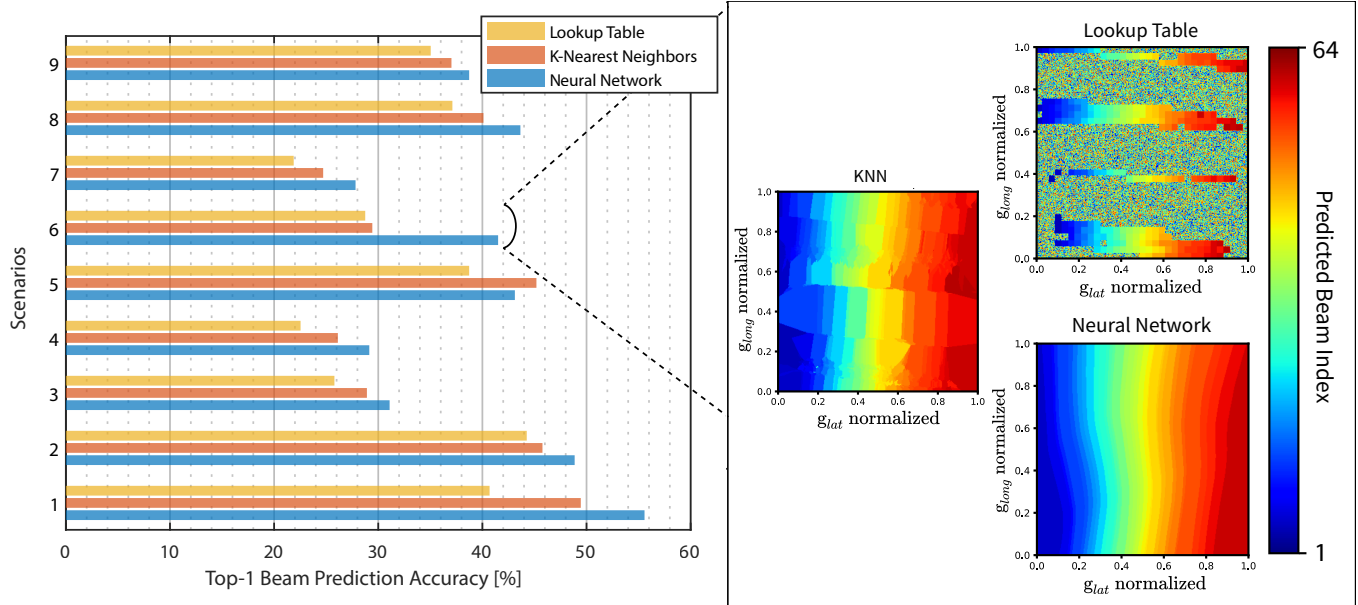
Normalization is a standard procedure in machine learning model training. The specific normalization procedure, however, depends on the data and application. Here, we normalize latitudes/longitudes with a min-max normalization on the absolute coordinates of the UE. We selected this approach after comparing several alternatives, such as using the relative coordinates to the BS, with divide-by-max normalizations that would not distort the scale of the data, and with the usage of polar coordinates, i.e., distance and angle. But the simple min-max normalization always provided the best results.

C. Data split

To train our models, we split the data of each Scenario as follows: 60% training, 20% validation, and 20% testing. It is a common practice to have equal splits for validation and test sets. We tested several similar data splits, and the influence on performance is minimal.

V. REAL-WORLD EXPERIMENTAL RESULTS

In this section, we present the answers to the questions stated in Section I. We derive answers based on simulations using our real-world dataset. To minimize the bias effects inherent in data shuffling and random weight initialization in the NN, we use 10 fixed randomization seeds and average the results across runs.



(a) Top-1 accuracy comparison on every Scenario.

(b) Scenario 6 prediction maps.

Fig. 2. Accuracy and beam prediction map comparison for the three considered algorithms, Lookup Table, KNN, and the Neural Network.

A. Algorithmic comparison

First, we compare the performance of the three adopted ML approaches and answer whether using a NN is excessive or justified. In Figure 2(a), we illustrate the top-1 accuracy for the three algorithms in all Scenarios. We see the NN consistently outperforming KNN and the LT. We can draw some insights into why this may happen by looking at Figure 2(b). It shows the output (color representing beam index) for each possible input. To generate it, we take the ML models trained for Scenario 6 and use them to predict the beams of 10 thousand uniformly spaced samples that cover our input space. We see that LT and KNN cannot generalize as well as the NN. This is justified because their input parameters (the number of bins/rows in the table and the number of neighbors in KNN), may not be optimal for all positions in a given scenario, depending heavily on the training data. Nevertheless, for each Scenario, we used the optimal setting for that parameter. Therefore, the NN is favored further, because it was up against the optimal versions of LT and KNN, and because it does not involve any scenario-specific optimization.

For systems that rely on ML models to narrow down the set of beams for over-the-air beam training, looking at top-1 prediction is not a complete and infallible way of comparing algorithms. In particular, algorithms may be performing comparatively well in top-1 but fail to generalize in top-3 or top-5 beam prediction accuracies. That is precisely represented in Figure 3 where we illustrate how the considered algorithms perform their five most confident guesses of the best beam. We see the NN returning more sensible second-guesses than KNN and LT. KNN and LT approaches fail to generalize to the depth of the NN because they do not consider data as a whole: KNN considers only some close neighbors and

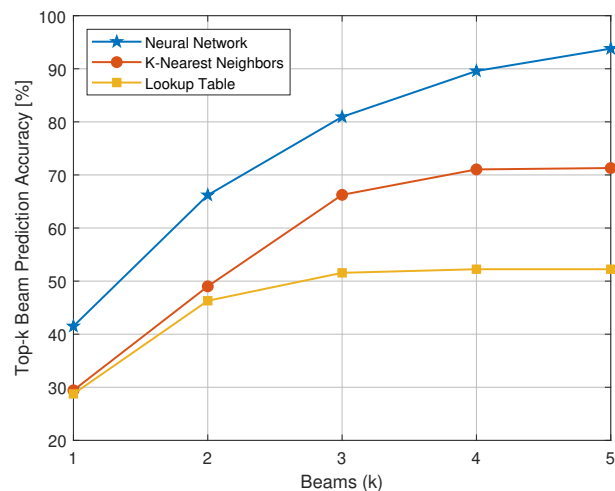


Fig. 3. Top-k accuracy comparison between algorithms for Scenario 6.

LT weighs samples only in a quantized cell. In opposition, the NN is a highly non-linear approach that implicitly uses information for all samples. After all, the network weights are adjusted for every training sample (or batch of samples), even if just infinitesimally. The NN is using and learning from more information than the KNN and LT counterparts, which justifies the quality of its generalizations over KNN and LT.

B. Factors that degrade performance

The results of the previous subsection show significantly different performances in each Scenario, and one naturally wonders why. Next, we group the key reasons in two categories, leaving the detailed analysis for follow-up work:

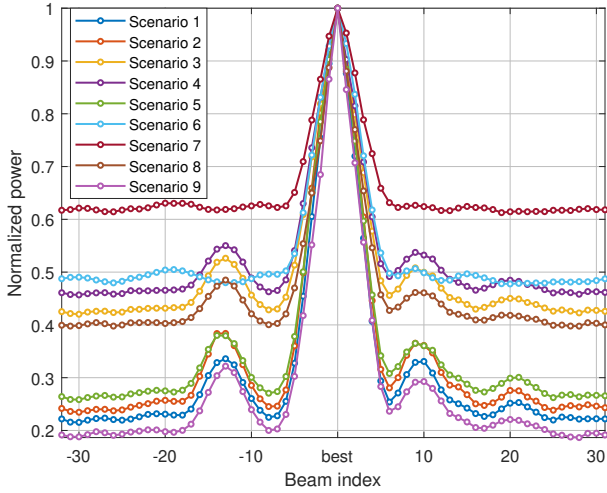


Fig. 4. Centered average beam power footprint: the time average of the received power using 64 different beams.

- **Noisy inputs:** due to GPS inaccuracies or unforeseen latency between the instant of measurement and instant of utilization of said measurement, the reported position can be differ from reality;
- **Noisy labels:** optimal beams may vary over time for the same spatial position, e.g., due to multipath fading, receiver noise, or overlapping of beam patterns. Moving scatterers may further unexpectedly affect propagation, e.g., causing blockages or unforeseen reflections.

The aforementioned factors lead to non-intuitive data that is harder to learn. If the position is noiseless and the labels are perfect then we may expect distinctively high prediction accuracy, which is consistent with the results based on synthetic data. We may postulate that low accuracies that we obtain with our real-world dataset were not predicted in literature because authors only considered input noise, which only in part accounts for performance degradation. To overcome this challenge, other auxiliary sources of information, possibly from other sensors, or more complex models and analysis techniques may further enhance the performance.

C. Meaningful performance metrics

The factors discussion in Section V-B affect both system performance and model accuracy, which are often treated as the same quantities. When several beams are received equally well (with similar receive power), selecting any of them results in almost equal performance. However, in terms of model prediction accuracy, not selecting the optimal beam results in clear degradation in this accuracy. To assess how power is distributed across beams, we plot the average power footprint for each Scenario in Figure 4. The power footprint consists of the received powers in all beams, and we average it across all samples taken in each Scenario. It tells us how much the accuracy might change across Scenarios without a direct impact on system performance, since Scenarios with a wider power spread across beams might present lower accuracy, without impacting in performance. We see that the power footprint varies noticeably, suggesting Scenarios with not

TABLE II
STATISTICS OF NN INFERENCE IN ALL SCENARIOS.
TOP-1 ACCURACY, POWER LOSS, AND 70%-POWER BEAMSET SIZE.

Scenario	Acc. [%]	P_L [dB]	$BS^{0.7}$
1	55.57	0.27	6.28
2	48.86	0.43	7.08
3	31.09	2.05	10.02
4	29.14	2.46	13.13
5	43.12	1.04	6.21
6	41.51	0.36	15.69
7	27.82	1.56	27.58
8	43.65	1.22	9.58
9	38.73	2.63	5.99

so similar accuracies may have similar performances, hence motivating the employment of more robust metrics.

Let us define a metric that targets system performance with more rigor. One such metric is the average power loss between prediction and ground truth, defined as

$$P_L = \frac{1}{K} \sum_{k=10}^K \log_{10} \left(\frac{P_{\hat{f}^*}^k - P_n}{P_{\hat{f}}^k - P_n} \right), \quad (5)$$

where P_n is the noise power of the Scenario, $P_{\hat{f}^*}^k$ is the power of the ground truth beam in sample k and $P_{\hat{f}}^k$ is the power with our predicted beam for sample k . The noise power is the average of the smallest power per sample, essentially, the lowest value of each Scenario in Figure 4.

Now, we capture the width of the power footprint plots into a single number we call the Beamset Size (BS), such that $BS^{(0.7)}$ consists of the number of beams within 70% of the power of the best beam. Our objective is to evaluate how inference accuracy and power relate to $BS^{(0.7)}$. We define $BS^{(0.7)} = \sum_{k=1}^K b_k^{(0.7)}$, with $b_k^{(0.7)} = \sum_{m=1}^M a_{k,m}^{(0.7)}$ and

$$a_{k,m}^{(0.7)} = \begin{cases} 1, & P_{f_m}^k \geq 0.7 P_{f^*}^k \\ 0, & \text{otherwise} \end{cases}, \quad (6)$$

where $P_{f_m}^k$ denotes the power received in sample k using the beamformer f_m . Now, we show in Table II the relation between the accuracy of each Scenario, the 70%-beamset size, and power loss. First and foremost, note that our solution achieves always less than 3dB power loss. Moreover, note what happens for similar power losses, which represent similar system-level performances. Take, for example, Scenarios 1 and 6, or Scenarios 7 and 8. Their accuracies vary substantially and in accordance with $BS^{(0.7)}$.

More generally, the columns of accuracy and power loss correlate well (-0.7), which makes sense since the system's performance is significantly dependent on the performance of the inference model. However, while accuracy correlates well with $BS^{(0.7)}$ (-0.6), power loss does not relate at all (0.005). We may conclude that P_L is a better system performance metric because it can see beyond the ML task performance since it is not affected by how wide the power footprint is.

TABLE III
TOP-1 ACCURACY COMPARISON WITH THE NUMBER OF BEAMS M.

Scenario	M=64	M=32	M=16	M=8
1	55.57	71.34	86.17	90.24
2	48.86	60.02	78.99	88.05
3	31.09	37.63	55.66	70.10
4	29.14	35.53	52.81	69.12
5	43.12	55.91	74.73	84.02
6	41.51	63.91	79.43	90.63
7	27.82	41.82	62.53	76.23
8	43.65	56.67	66.72	76.97
9	38.73	49.42	66.75	76.22
Average	39.9	52.5	69.3	80.2

D. Accuracy depends on the size of the codebook

Although we proved that accuracy might not entirely reflect the overall system performance, it still could allow us to compare how well a model is performing. And we should note that the model performance also depends on how many categories it needs to classify. In particular, if the model needs to differentiate between fewer beams, the task is more manageable, and vice-versa. In Table III, we show quantitatively how model accuracy varies with the number of beams considered. Although values depend to a large degree on the considered Scenario, classifying the best beam among fewer candidates always leads to higher accuracies.

E. How much overhead do GPS positions save?

If we define overhead savings as the reduction in the number of beams that require training, then we can guarantee an overhead level that depends only on the reliability (or outage probability) we want in the ML task. The reliability is the confidence we have that a specific set of beams contains the best. Therefore, the higher the confidence, the more beams our set should have, and the lowest our overhead savings.

Let us assume that all 64 beams would require training for the system to discover the ideal candidate. Then our overhead savings with a reliability of at least 90%, $\alpha_{OH}^{(90)}$, is given by

$$\alpha_{OH}^{(90)} = 1 - \frac{b^{(90)}}{M} \quad (7)$$

where $b^{(90)}$ is the minimum number of beams (on average) needed so their likelihood probabilities sum to more than 90%, and M is the codebook size. For $M = 64$, we show in Figure 5 the overhead savings for typical reliability values. For example, with an reliability of 90% (outage probability of 10%), we may save between 81% and 95% of training overhead, depending on the Scenario. And for 99% reliability, our approach saves 66% overhead on average.

VI. CONCLUSIONS

In this work, we assessed how much real-world position data could help in reducing the signaling overhead. First, we evaluated which algorithm yields the best performance. We verified that the NN consistently outperforms the optimally

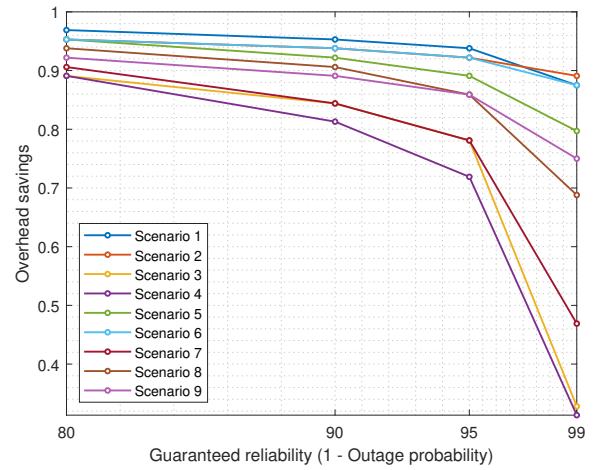


Fig. 5. Overhead savings in all adopted DeepSense 6G scenarios as a function of outage probability.

tuned lookup table and KNN. Not only does it exceed in top-1 performance, but it also generalizes visibly better, achieving increasingly superior top-k performance. Second, we identified the causes of performance deterioration which we classified to input noise and label noise. Then, we demonstrated how power loss could be a better system performance metric since it is directly related to the end communication objectives. Our results show that the proposed position-aided beam prediction solution resulted in power losses that are less than 3dB compared to the ideal ground-truth beams in all analyzed real-world scenarios. In terms of beam training overhead, we showed that more than 70% saving compared to exhaustive search is feasible while guaranteeing more than 95% beam prediction accuracy. These results highlight the potential of leveraging position data for aiding the beam management tasks in beyond 5G communication systems and draw insights into several research directions that could further improve the performance in real-world deployments.

REFERENCES

- [1] T. S. Rappaport, Y. Xing, O. Kanhere, S. Ju, A. Madanayake, S. Mandal, A. Alkhateeb, and G. C. Trichopoulos, "Wireless communications and applications above 100 ghz: Opportunities and challenges for 6g and beyond," *IEEE Access*, vol. 7, pp. 78 729–78 757, 2019.
- [2] I. Mavromatis, A. Tassi, R. J. Piechocki, and A. Nix, "mmWave system for future its: A MAC-layer approach for V2X beam steering," in *2017 IEEE 86th Vehicular Technology Conference (VTC-Fall)*, 2017, pp. 1–6.
- [3] S. Rezaie, C. N. Manchón, and E. de Carvalho, "Location- and orientation-aided millimeter wave beam selection using deep learning," in *IEEE International Conference on Communications (ICC)*, 2020.
- [4] Y. Heng and J. G. Andrews, "Machine learning-assisted beam alignment for mmwave systems," *IEEE Transactions on Cognitive Communications and Networking*, pp. 1–1, 2021.
- [5] Y. Wang, A. Klautau, M. Ribero, M. Narasimha, and R. W. Heath, "mmWave vehicular beam training with situational awareness by machine learning," in *2018 IEEE Globecom Workshops*, 2018, pp. 1–6.
- [6] A. Alkhateeb, G. Charan, T. Osman, A. Hredzak, and N. Srinivas, "DeepSense 6G: Large-scale real-world multi-modal sensing and communication datasets," *to be available on arXiv*, 2022. [Online]. Available: <https://www.DeepSense6G.net>
- [7] M. Joao, github.com/jmoraispk/Position-Beam-Prediction, 2021.
- [8] D. P. Kingma and J. Ba, "Adam: A method for stochastic optimization," 2017.